Biochemistry and Biophysics Reports 9 (2017) 245–256

Contents lists available at ScienceDirect

Biochemistry and Biophysics Reports

journal homepage: www.elsevier.com/locate/bbrep

Flecainide ameliorates arrhythmogenicity through NCX flux in Andersen-Tawil syndrome-iPS cell-derived cardiomyocytes

Yusuke Kuroda[a,b,c], Shinsuke Yuasa[a,*], Yasuhide Watanabe[d], Shogo Ito[a], Toru Egashira[a], Tomohisa Seki[a], Tetsuhisa Hattori[e], Seiko Ohno[e,f], Masaki Kodaira[a], Tomoyuki Suzuki[a,b,c], Hisayuki Hashimoto[a], Shinichiro Okata[a], Atsushi Tanaka[a], Yoshiyasu Aizawa[a], Mitsushige Murata[a,g], Takeshi Aiba[h], Naomasa Makita[i], Tetsushi Furukawa[j], Wataru Shimizu[k], Itsuo Kodama[b], Satoshi Ogawa[a], Norito Kokubun[l], Hitoshi Horigome[m], Minoru Horie[e], Kaichiro Kamiya[b], Keiichi Fukuda[a]

[a] Department of Cardiology, Keio University School of Medicine, Tokyo, Japan
[b] Department of Cardiovascular Research, Research Institute of Environmental Medicine, Nagoya University, Aichi, Japan
[c] Department of Cardiology, Nagoya University Graduate School of Medicine, Aichi, Japan
[d] Division of Pharmacological Science, Department of Health Science, Hamamatsu University School of Medicine, Shizuoka, Japan
[e] Department of Cardiovascular Medicine, Shiga University of Medical Science, Shiga, Japan
[f] Center for Epidemiologic Research in Asia, Shiga University of Medical Science, Shiga, Japan
[g] Department of Laboratory Medicine, Keio University School of Medicine, Tokyo, Japan
[h] Division of Arrhythmia and Electrophysiology, Department of Cardiovascular Medicine, National Cerebral and Cardiovascular Center, Osaka, Japan
[i] Department of Molecular Pathophysiology-1, Nagasaki University Graduate School of Biomedical Sciences, Nagasaki, Japan
[j] Department of Bio-informational Pharmacology, Medical Research Institute, Tokyo Medical and Dental University, Tokyo, Japan
[k] Department of Cardiovascular Medicine, Nippon Medical School, Tokyo, Japan
[l] Department of Neurology, Dokkyo Medical University, Tochigi, Japan
[m] Department of Child Health, Faculty of Medicine, University of Tsukuba, Tsukuba, Japan

ARTICLE INFO

Keywords:
Cardiomyocyte
Arrhythmia
Andersen-Tawil syndrome
iPS cell

ABSTRACT

Andersen-Tawil syndrome (ATS) is a rare inherited channelopathy. The cardiac phenotype in ATS is typified by a prominent U wave and ventricular arrhythmia. An effective treatment for this disease remains to be established. We reprogrammed somatic cells from three ATS patients to generate induced pluripotent stem cells (iPSCs). Multi-electrode arrays (MEAs) were used to record extracellular electrograms of iPSC-derived cardiomyocytes, revealing strong arrhythmic events in the ATS-iPSC-derived cardiomyocytes. Ca^{2+} imaging of cells loaded with the Ca^{2+} indicator Fluo-4 enabled us to examine intracellular Ca^{2+} handling properties, and we found a significantly higher incidence of irregular Ca^{2+} release in the ATS-iPSC-derived cardiomyocytes than in control-iPSC-derived cardiomyocytes. Drug testing using ATS-iPSC-derived cardiomyocytes further revealed that antiarrhythmic agent, flecainide, but not the sodium channel blocker, pilsicainide, significantly suppressed these irregular Ca^{2+} release and arrhythmic events, suggesting that flecainide's effect in these cardiac cells was not via sodium channels blocking. A reverse-mode Na^{+}/Ca^{2+}exchanger (NCX) inhibitor, KB-R7943, was also found to suppress the irregular Ca^{2+} release, and whole-cell voltage clamping of isolated guinea-pig cardiac ventricular myocytes confirmed that flecainide could directly affect the NCX current (I_{NCX}). ATS-iPSC-derived cardiomyocytes recapitulate abnormal electrophysiological phenotypes and flecainide suppresses the arrhythmic events through the modulation of I_{NCX}.

1. Introduction

In 1971, Andersen et al. [1] reported a patient with intermittent muscular weakness, extrasystoles, and multiple developmental anomalies. Then in 1994, Tawil et al. [2] denoted a novel and distinct clinical syndrome showing potassium-sensitive periodic paralysis, cardiac arrhythmia, and dysmorphic features as Andersen syndrome, warranting attention due to the potentially lethal cardiac arrhythmic events.

* Correspondence to: Department of Cardiology, Keio University School of Medicine, 35 Shinanomachi Shinjuku-ku, Tokyo 160-8582, Japan.
E-mail address: yuasa@keio.jp (S. Yuasa).

http://dx.doi.org/10.1016/j.bbrep.2017.01.002
Received 23 August 2016; Received in revised form 9 December 2016; Accepted 10 January 2017
Available online 11 January 2017

Thereafter, Andersen syndrome was generally renamed as Andersen-Tawil syndrome (ATS). Early reports also described ATS patients with QT interval prolongation, and consequently ATS was proposed as long QT syndrome type 7 (LQTS7) [3]. However, accumulating subsequent findings showed that QT interval prolongation is not a common feature of ATS, although prominent U wave and QU interval prolongation can be hallmarks of ATS, distinguished it from long QT syndrome [4]. Approximately 40% of ATS patients show cardiac arrhythmias on the baseline electrocardiogram, half of which are diagnosed as non-sustained ventricular tachycardia, and 3% of ATS patients show Torsade de pointes [4]. However, a French cohort showed that a severe clinical presentation with a very high rate of ventricular arrhythmias might be unrelated to the fatal arrhythmic prognosis of ATS patients [5].

Several clinical cues and case reports of ATS have provided hints for future standardized treatments. Exercise is an important trigger of ventricular tachyarrythmia and syncope in some patients with ATS, therefore patients are commonly treated with beta-blocker therapy [6]. Other drugs such as flecainide, calcium blockers, acetazolamide, and amiodarone have been proposed by anecdotal experiences [7–9]. An implantable cardiac defibrillator (ICD) is often necessary when patients showed fatal cardiac arrhythmias [10]. However, the rarity of ATS hampers the analytical interrogation of clinical data and thus the development of effective treatments, and it remains unclear who should be treated, as well as when and how [11,12].

ATS is an autosomal dominant genetic or sporadic disorder and has been linked to mutations in *KCNJ2*, a genotype labeled as ATS type 1 (ATS1) [13]. Patients with such mutations in *KCNJ2* accounts for about 70% of ATS cases, with the remaining 30% of cases labeled as type 2 (ATS2), for which the genetic cause remains unknown [14]. *KCNJ2* encodes for a voltage-gated, inward-rectifying potassium channel (Kir2.1) that contributes to the cardiac inward rectifier current I_{K1}. Most *KCNJ2* mutations in ATS1 cause loss of function and dominant-negative suppression of the Kir2.1 channel function, leading to less I_{K1} [15,16]. Most of the electrophysiological studies have used a heterologous expression system, with human mutated genes in non-human/non-cardiac cells, such as Xenopus oocyte and HEK293 cells. I_{K1} is present in human ventricular and atrial cardiomyocytes and might play a major role in repolarizing the action potential and stabilizing the resting potential in humans [17,18]. Simulation studies suggest that a reduction in I_{K1} during the terminal phase of repolarization and during diastole would induce delayed after-depolarizations (DADs) and spontaneous arrhythmias [3,19]. To elucidate the pathophysiological function of mutated genes in the human heart, patient cardiomyocytes can be compared to human control cardiomyocytes. However, human cardiomyocytes from living patients are not an easily obtained or abundant enough tool for basic research. Reprogramming of human somatic cells into induced pluripotent stem cells (iPSCs) potentially enables us to generate patient-specific, disease-specific iPSCs as in vitro genetic disease models. To this end, several studies have yielded disease models using patient-specific iPSCs [20–24].

This study sought to establish a model for ATS using patient-specific iPSCs, to elucidate the pathogenesis of ATS and search for potential drug candidates for therapy. We thus generated iPSCs from three ATS patients carrying one of the *KCNJ2* mutations (R218W, R218Q, R67W, respectively). Multi-electrode array (MEA) analysis revealed strong arrhythmic events in these ATS-iPSC-derived cardiomyocytes, and Ca^{2+} imaging unveiled a highly irregular Ca^{2+} release. Drug testing subsequently revealed that both of these effects were significantly suppressed in the ATS-iPSC-derived cardiomyocytes by flecainide and a reverse-mode Na^+/Ca^{2+} exchanger (NCX) inhibitor. Finally, whole-cell voltage clamping of isolated guinea-pig ventricular cardiomyocytes showed that flecainide could directly affect I_{NCX}. Our results indicate that ATS-iPSC-derived cardiomyocytes could recapitulate abnormal electrophysiological phenotypes and thus might serve as a useful model for exploring disease mechanisms and drug screening.

2. Materials and methods

2.1. Patient consent

All subjects provided informed consent for blood testing for genetic abnormalities associated with ATS. The Ethics Committee of Keio University approved the isolation and use of patient and control somatic cells for iPSC studies (approval no. 20–92–5), which was performed only after the patients and controls had provided written informed consent. Our study also conforms with the principles outlined in the Declaration of Helsinki (Cardiovascular Research 1997;35:2-3) for use of human tissue or subjects. Patient 1 is 10 years old, male with a KCNJ2 R218W mutation. Patient 2 is 27 years old, male with a KCNJ2 R67W mutation. Patient 3 is 47 years old, male with a KCNJ2 R218Q mutation. Control 1 is 29 years old, male and control 2 is 24 years old, male.

2.2. Human iPSCs generation

The iPSCs were established from T lymphocytes with Sendai virus encoding *OCT3/4, SOX2, KLF4,* and *c-MYC* [25,26]. Briefly, peripheral blood mononuclear cells (PBMCs) were collected and transferred at 1.5×10^6 cells per well to a fresh anti-CD3 antibody-coated 6-well plate, and incubated for an additional 24 h. Then, solutions containing the Sendai virus vectors individually carrying each of *OCT3/4, SOX2, KLF4,* and *c-MYC* were added at 10 MOI. After 24 h of infection, the medium was changed to fresh KBM 502 medium (KOHJIN BIO, Saitama, Japan), and the cells were collected and split at 5×10^4 cells into 10 cm plates pre-seeded with mouse embryonic fibroblasts (MEFs). After an additional 24 h of incubation, the medium was changed to hiPSC medium supplemented with 4 ng/ml basic fibroblast growth factor (bFGF). Approximately 20–30 days after infection, iPSC colonies appeared and were picked up. Sendai virus vectors carrying the same four specific transcriptional factors independently were commercially obtained (Life Technologies; CytoTune-iPS reprogramming kit).

2.3. Cell culture

Human iPSCs were maintained on irradiated MEF feeder cells in hiPSC culture medium: 80% DMEM/F12 (Sigma-Aldrich, MO, USA), 20% KO Serum Replacement (Invitrogen, CA, USA), 4 ng/ml bFGF (WAKO, Osaka, Japan), 2 mM L-glutamine (Invitrogen), 0.1 mM non-essential amino acids (Sigma-Aldrich), 0.1 mM 2-mercaptoethanol, 50 U/ml penicillin, and 50 mg/ml streptomycin (Invitrogen). The hiPSC medium was changed every 2 days, and the cells were passaged using 1 mg/ml collagenase IV (Invitrogen) every 5–7 days.

2.4. Teratoma formation

To confirm pluripotency *in vivo*, teratoma formation was assessed in accordance with the Institutional Animal Care and Use Committee of Keio University. Approximately $1–2\times10^6$ iPSCs were injected into the testis of anesthetized immune-compromised NOD-SCID mice (CREA-Japan, Tokyo, Japan). At 10–12 weeks after the injection, mice were euthanized and the teratomas were excised, fixed overnight in formalin, embedded in paraffin, and analyzed by haematoxylin-eosin staining. The mice were anesthetized using a mixture of ketamine (50 mg/kg), xylazine (10 mg/kg), and chlorpromazine (1.25 mg/kg). The adequacy of anesthesia was monitored by heart rate, muscle relaxation, and the loss of sensory reflex responses, i.e., nonresponsive to tail pinching. The investigation conforms with the Guide for the Care and Use of Laboratory Animals published by the US National Institutes of Health (publications number 23–80 revised in 2011) and was approved by university review board in Keio University.

2.5. Genome sequencing

DNA sequencing was used to confirm the mutations in patient-derived iPSCs. Genomic DNA was isolated using a Gentra Puregene Cell Kit (Qiagen, Venlo, Netherland) and the region encoding the mutation was amplified by polymerase chain reaction (PCR). The PCR product was electrophoresed on a 1% agarose gel and purified using a Wizard SV Gel and PCR Clean-Up System (Promega, WI, USA). The purified PCR product was sequenced with original primers (Supplementary Table 1) [27].

2.6. In vitro *cardiomyocyte differentiation*

Differentiation of iPSCs to cardiomyocytes was induced via embryoid bodies (EBs) [28,29]. iPSCs colonized on MEF feeders were detached by 1 mg/ml type IV collagenase (Invitrogen), and suspended on ultra-low attachment plates (Corning, NY, USA) with differentiation medium, consisting of 80% Minimum Essential Medium Alpha Medium (Gibco, CA, USA), 2 mM L-glutamine (Invitrogen), 0.1 mM non-essential amino acids (Sigma-Aldrich), 0.1 mM 2-mercaptoethanol, 50 U/ml penicillin and 50 mg/ml streptomycin (Invitrogen), and 20% fetal bovine serum (Gibco). During suspension culture, the medium was changed every 2 days during the first week, after then every 4–5 days. For immunofluorescence and Ca^{2+} imaging, single cardiomyocytes were obtained by dissociating spontaneously beating EBs using 0.25% trypsin (Invitrogen) and 1 mg/ml type IV collagenase (Invitrogen). Cardiomyocytes were plated on fibronectin (Sigma-Aldrich)-coated dishes. All assays were performed using beating EBs and cardiomyocytes, which were cultured 60–80 days after differentiation. All experiments we have done include the mixed data from 2 clones of each 2 control individual and 2 clones of each patient-derived iPSC.

2.7. Immunofluorescence

Colonies of undifferentiated human iPSCs plated on MEF feeder cells and cardiomyocytes plated on fibronectin-coated dishes were fixed with 4% paraformaldehyde (MUTO Pure Chemicals, Tokyo, Japan) for 30 min at 4 °C. After fixation, cells were permeabilized with 1% Triton X-100 and blocked with ImmunoBlock (DS Pharma Biomedical, Osaka, Japan). Specimens were incubated at 4 °C overnight with each of the following primary antibodies: anti-OCT3/4 (Santa Cruz, CA, USA), anti-NANOG (Abcam, Camb, UK), anti-SSEA3 (Millipore, MA, USA), anti-Tra1-81 (Millipore), anti-TroponinT (Thermo Scientific, MA, USA), anti-alpha-actinin (Sigma-Aldrich), anti-GATA4 (Santa Cruz) and anti-ANP (Santa Cruz). Preparations were incubated with secondary antibodies for 1 h at room temperature. Nuclei were counterstained with 50 ng/ml 4′,6′-diamidino-2-phenylindole (DAPI; Invitrogen). Fluorescent signals were detected using a fluorescence laser microscope equipped with 1.5×10^5 pixels charged coupled device (CCD) camera (BZ-9000, Keyence, Osaka, Japan).

2.8. Drug testing

Isoproterenol hydrochloride (Tokyo Chemical Industry, Tokyo, Japan), Flecainide acetate salt (Sigma-Aldrich), Pilsicainide hydrochloride (Sigma-Aldrich), KB-R7943 (Sigma-Aldrich), SEA0400 (MedChem Express, NJ, USA) and JTV519 (Sigma-Aldrich) were used for the drug testing assays. In drug testing experiments, we added prewarmed medium containing each drug, mildly by pipetting and mixed well gently. The temperature of medium was maintained at 37 °C during experiment.

2.9. Multi-electrode array recordings

A multi-electrode array (MEA) recording system (Multichannel Systems, Reutlingen, Germany) was used to characterize the electrophysiological properties of human iPSC-derived cardiomyocytes. The spontaneously beating EBs were plated on fibronectin-coated MEA plates and incubated at 37 °C. The extracellular electrograms were recorded in DMEM/HEPES (D5796; Sigma-Aldrich) at 37 °C, and the obtained data were subsequently analyzed with MC_Rack (Multichannel Systems). The extracellular electrograms were used to determine field potential duration (FPD) and detect arrhythmic events. FPD was defined as the time interval between the initial deflection of the field potential and its return to baseline. FPD measurements were normalized (cFPD) to the rate using Bazett's correction formula: $cFPD=FPD/(RR\ interval)^{1/2}$.

2.10. Ca^{2+} imaging

Cardiomyocytes were placed on 35 mm glass-bottom dishes and loaded with 5 μM Fluo-4 AM (Invitrogen) in Tyrode's solution for 30 min at 37 °C. Ca^{2+} imaging was performed with a confocal microscope (LSM 510 Duo, Carl Zeiss, Jena, Germany) using a ×40 objective (NA=0.75). Line scans were acquired at a sampling rate of 2 ms/line (total of 10,000 times for a 20 s recoding). Cardiomyocytes spontaneously beating and electrically stimulated at 1 Hz were analyzed.

2.11. Action potential measurement in iPSC-derived cardiomyocytes

Cardiomyocytes were isolated from the spontaneously beating EBs by enzymatic dissociation, and action potentials were recorded in own beating condition by a conventional whole-cell configuration of patch-clamp techniques at 37 °C, using an Axopatch 200B patch clamp amplifier and a Digidata 1550 digitizer (Axon Instruments, Foster City, CA, USA). Action potentials were evoked by 2 ms supra-threshold current pulses at 1 Hz in the current-clamp mode. Pipettes were filled with the following solution (in mM): KCl 20, L-Glutamic acid monopotassium salt 120, NaCl 10, HEPES 10 (pH 7.2 with KOH), while Tyrode's solution contained (in mM): NaCl 140, KCL5.4, $CaCl_2$ 1.8, $MgCl_2$ 0.33, NaH_2PO_4 5.5, glucose 5.5, HEPES 5.0 (pH7.4 with NaOH). Ventricular-type action potentials are distinguished by the presence of a marked plateau phase and an APD_{90}/APD_{50} ratio up to 1.3 [30].

2.12. Patch clamp experiment in the guinea-pig ventricular cardiomyocytes

Patch-clamp experiment was performed under the regulation of the Animal Research Committee of the Hamamatsu University School of Medicine. Single ventricular cells were isolated from guinea-pig heart by enzymatic dissociation. I_{NCX} was recorded by loading Na^+ and Ca^{2+} in both the intracellular and extracellular solutions, as previously described [31]. The external solution was maintained at 36 °C ± 0.5 °C. I_{NCX} was recorded with a patch-clamp amplifier (TM-1000; Act ME, Tokyo, Japan), filtered at a 2.5-kHz bandwidth, and the series resistance was compensated. Data were stored using pCLAMP8 software (Axon Instruments). The current–voltage (I–V) relationship was obtained by ramp pulses from the holding potential of −60–0 mV, to −140 mV, and then back to −60 mV at a constant rate of 640 mV s^{-1}. The descending limb (from 0 to −140 mV) was plotted in the I–V relationship without capacitance compensation. The pipette resistance was 2–3 MΩ when filled with the pipette solution. The control external solution contained ouabain, nifedipine, Cs^+, and ryanodine to block the Na^+/K^+ pump current, I_{Ca}, K^+ currents, and Ca^{2+} release channels of the sarcoplasmic reticulum, respectively. The animal procedures were performed conform the NIH guidelines (Guide for the care and use of laboratory animals). Adult guinea pig was anesthetized by 100 mg/kg sodium thiopental (Sigma-Aldrich, St Louis, MO, USA) and euthanized by cervical dislocation.

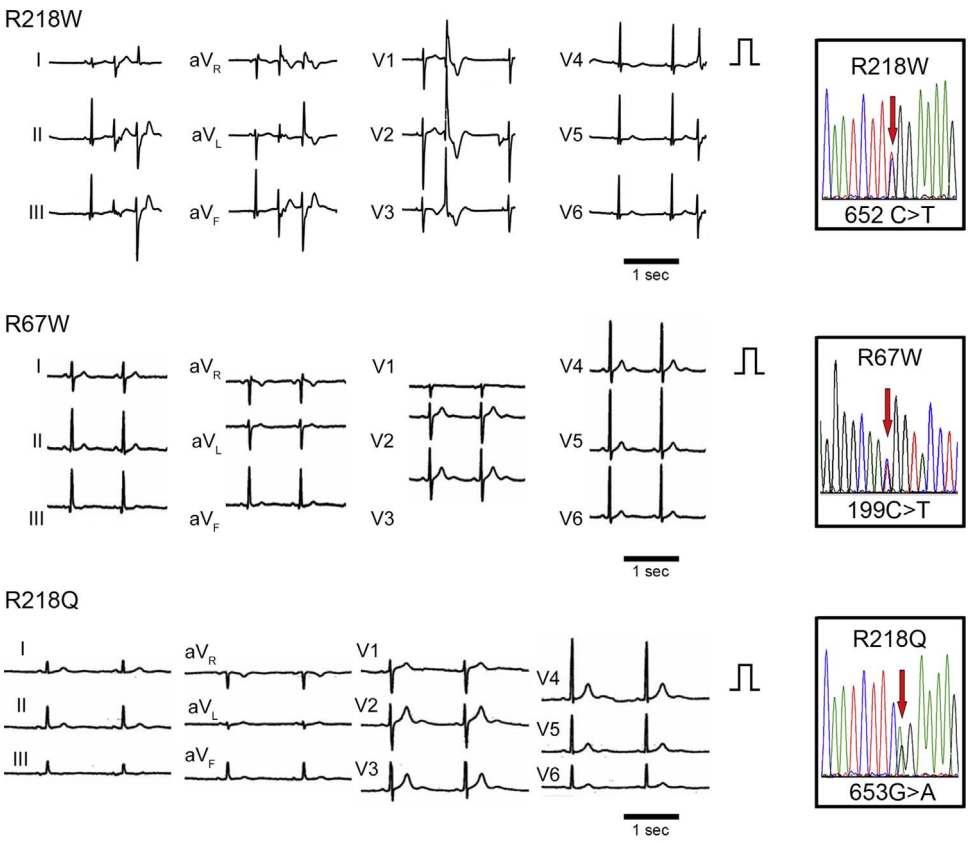

Fig. 1. Electrocardiograms of patients with ATS, Electrocardiograms from the patients with ATS during sinus rhythm. QT and QTc intervals: QT interval/(RR interval)$^{1/2}$ are 480 ms and 462 ms (R218W), 400 ms and 400 ms (R67W), 420 ms and 383 ms (R218Q), respectively. QU and QUc intervals: QU interval/(RR interval)$^{1/2}$ are 680 ms and 654 ms (R218W), 680 ms and 680 ms (R67W), 720 ms and 657 ms (R218Q), respectively. The normal QTc interval is < 440 ms. The boxes on the right represent the sequence analysis of genomic *KCNJ2* from each iPSC.

2.13. Statistical analyses

Every data shown as "ATS" was obtained by using equal proportion of the data from six ATS-iPSC lines. Values are presented as the mean ± SEM. The significance of differences between two means was evaluated by unpaired and paired *t*-tests. Chi-square test and Fisher's exact probability test was used for comparisons between groups. Comparisons between more than two groups were determined by ANOVA followed by Tukey-kramer test. $P < 0.05$ was considered significant. *P < 0.05. **P < 0.01. †P < 0.001.

3. Results

3.1. Generation of Andersen-Tawil syndrome-iPSCs

We selected three unrelated patients with ATS. Each patient has a mutation at *KCNJ2*, R218W, R67W, R218Q, respectively, which were previously characterized. All cases showed prominent U waves on their electrocardiogram (Fig. 1). Case 1 (R218W) shows frequent premature ventricular contractions (PVCs) by electrocardiogram, while Case 2 (R67W) and Case 3 (R218Q) have a history of periodic paralysis (Supplementary Table 2). As controls, we used two populations of iPSCs derived from healthy volunteers, including a previously characterized control iPSC line [20,25,32]. After normal karyotypes of generated iPSCs were examined, each iPSC was further investigated. The generated ATS-iPSCs and control-iPSCs showed appropriate stem cell marker expression (Fig. 2a, Supplementary Fig. 1) as well as multipotency, based on teratoma formation involving tissues derived from all three germ layers (Fig. 2b, Supplementary Fig. 2). Subsequently, cardiomyocytes were differentiated from the iPSCs by EB formation, and immunostaining revealed that these cells expressed cardiomyocyte-specific markers, α-actinin, atrial natriuretic peptide (ANP), cardiac troponin T (cTnT), and GATA4, and showed normal cardiomyocyte cellular structure (Fig. 2c, Supplementary Fig. 3).

3.2. Electrophysiological characterization of ATS-iPSC-derived cardiomyocytes under baseline conditions

To investigate the electrophysiological properties of the derived cells, we used an MEA system to measure the surface electrogenic activities of cell clusters. The MEA analyses revealed that control-iPSC- and ATS-iPSC-derived EBs showed similar rhythmic electrical activity (Fig. 3a), with no significant difference in spontaneous beating rate (Fig. 3b). The field potential duration (FPD) in MEA analysis is analogous to the QT interval in a surface electrocardiogram [20], and there was no significant difference in the cFPD (normalized for beating frequency) between control-iPSC- and ATS-iPSC-derived EBs (Fig. 3c). These data are consistent with previous evidence of no significant difference in QT interval between control and ATS patients [4]. Next we investigated the action potentials electrically captured at 1 Hz in control- and ATS-iPSC-derived cardiomyocytes. We observed typical ventricular-type action potentials (Figs. 3d, 3e, 3f, 3g), while phase 3 repolarization was mildly decelerated in the ATS-iPSC-derived cardiomyocytes, although there was no significant difference in action potential duration $(APD)_{50}$ and APD_{90} compared to control-derived cells (Fig. 3h, i). Additionally, there were no significant differences in maximum diastolic potential (MDP) (Fig. 3j).

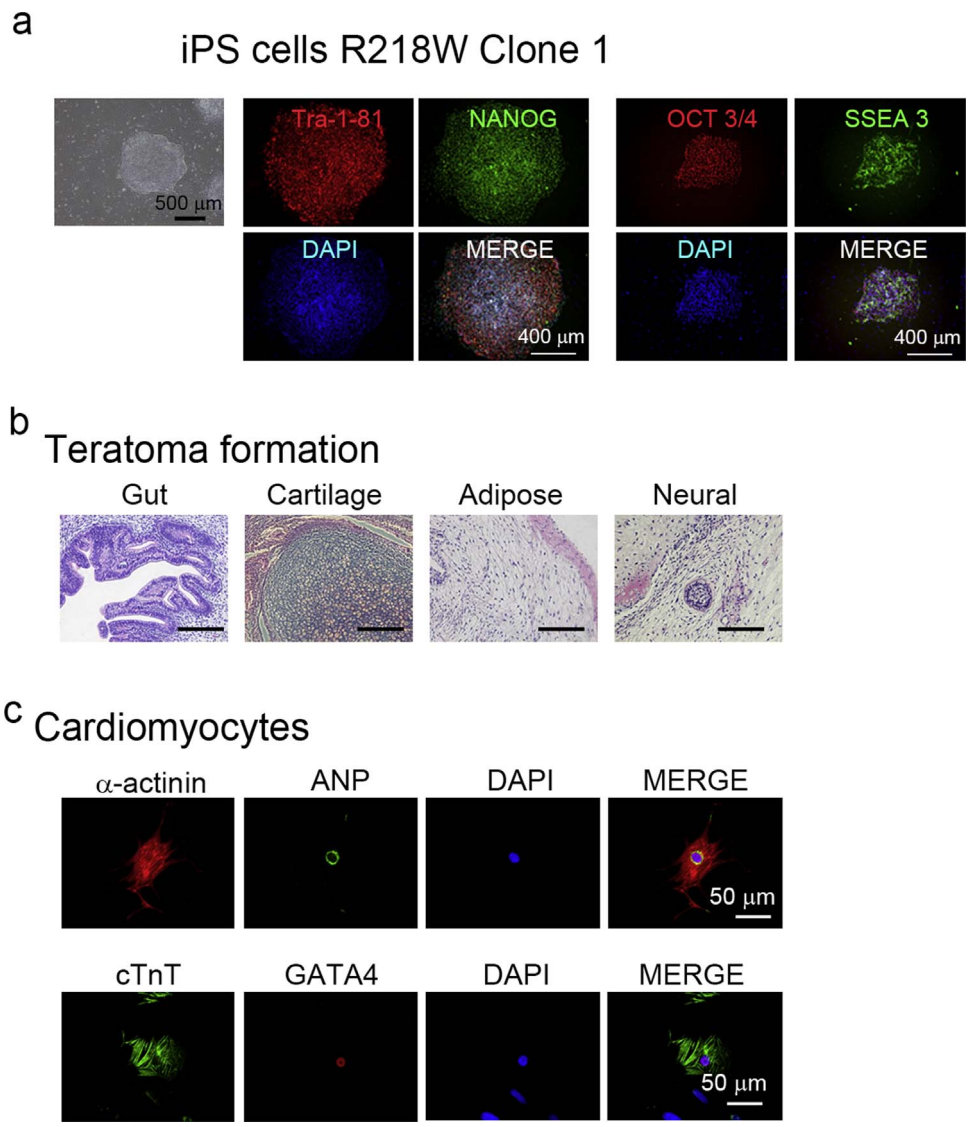

Fig. 2. Generation of iPSCs from three patients with ATS, a. Immunofluorescence staining for stem cell markers (Tra1-81, NANOG, OCT3/4, and SSEA3) in iPSCs of ATS case (R218W). Nuclei were counterstained with DAPI. b. Microscopic observation of teratoma sections, showing tissue structures resembling gut (endoderm), cartilage (mesoderm), adipose (mesoderm), and neural tissue (ectoderm). c. Immunofluorescence staining for cardiomyocyte markers (α-actinin, ANP, cardiac troponin T (cTnT), and GATA4) in control- and ATS-iPSC-derived cardiomyocytes. Nuclei were counterstained with DAPI.

3.3. Flecainide has a therapeutic potential on ATS-iPSC-derived cardiomyocytes

Accumulating clinical information suggests that exercise and catecholamine stimulation can be triggers of ventricular tachyarrythmia in patients with ATS [6]. Thus we next examined the effect of catecholamine on iPSC-derived cardiomyocytes by MEA analyses. In control-iPSC-derived cardiomyocytes, isoproterenol administration increased the beating rate, but not the incidence of arrhythmic events (Fig. 4a). In ATS-iPSC-derived cardiomyocytes, isoproterenol administration increased the beating rate and induced arrhythmic events (Fig. 4b, Supplementary Fig. 4b). We defined the arrhythmic event in this study as the surface electrogenic activity which shows at least one of following characters, different shape, different polarity, different timing from basic rhythm. The incidence of beating EBs with arrhythmic events was significantly increased in ATS-iPSC-derived cardiomyocytes (Fig. 4c, Supplementary Fig. 4a). Some reports have implicated the therapeutic potential of flecainide for controlling arrhythmic events in ATS patients, although the therapeutic mechanisms underlying such an effect remain elusive. In MEA analyses, flecainide reduced the incidence of the EBs with arrhythmic events (Figs. 4b, 4d, Supplementary Fig. 4b–d).

3.4. Abnormal calcium transient in ATS-iPSC-derived cardiomyocytes

To further investigate the mechanisms underlying the arrhythmogenicity of ATS, we analyzed the Ca^{2+}-handling properties of iPSC-derived single cardiomyocytes, using fluorescent Ca^{2+} imaging. In spontaneously self-beating cardiomyocytes, the ATS-iPSC-derived cardiomyocytes often exhibited irregular Ca^{2+} release compared to control-iPSC-derived cardiomyocytes (Fig. 5a, Supplementary Fig. 5a), with the rate of cardiomyocytes with irregular Ca^{2+} release significantly increased in ATS-iPSC-derived cardiomyocytes (Fig. 5b). To measure the precise properties of Ca^{2+} dynamics, the beating of iPSC-derived cardiomyocytes was electrically captured at 1 Hz (Fig. 5c, Supplementary Fig. 5b). The intensity (ΔF/F0) was increased in ATS-iPSC-derived cardiomyocytes compared to controls (Fig. 5d). However, there was no significant difference in time to peak, time to 90% decay of the Ca^{2+} transient (CaT_{90}), and τ of Ca^{2+} transient decline

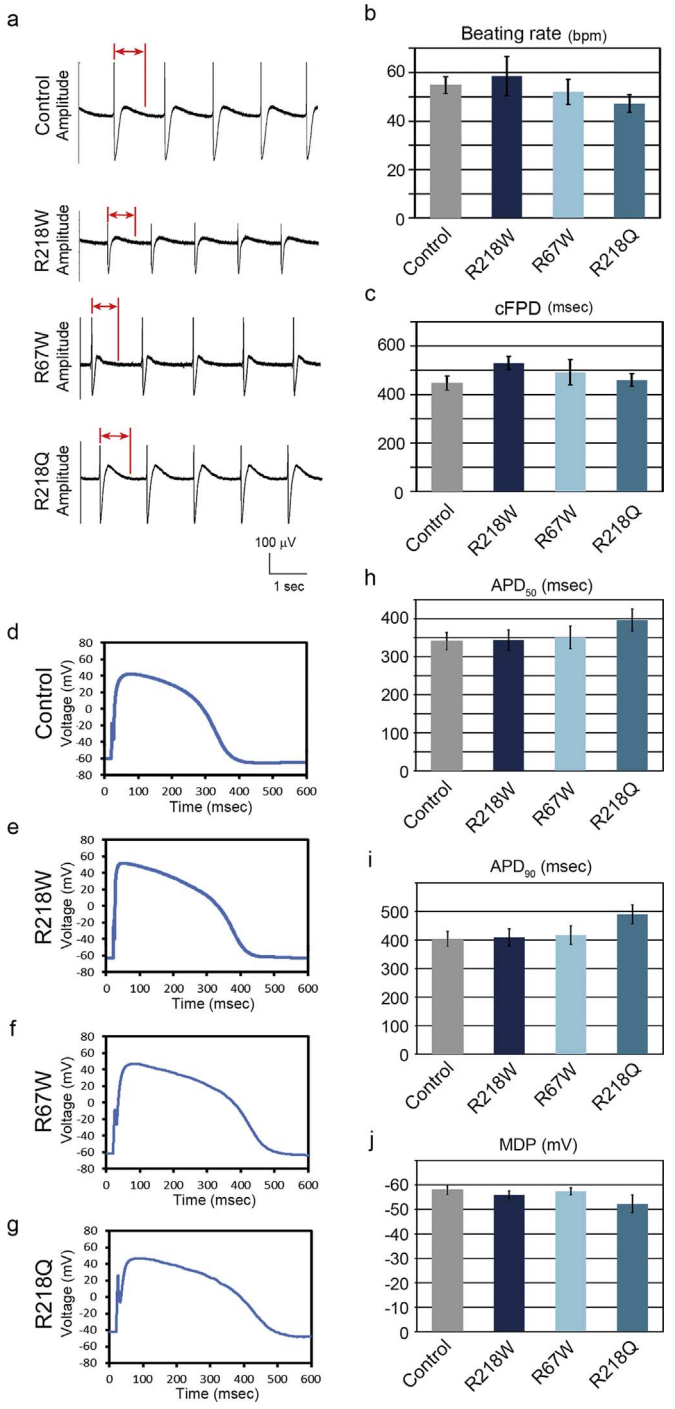

Fig. 3. Electrophysiological features of ATS-iPSC-derived cardiomyocytes, a. Representative MEA recordings from the control- and ATS-iPSC-derived beating EBs. The bidirectional red arrows indicate FPD. b. Beating rate of the control- (n=14) and ATS-iPSC-derived EBs (n=12–14) at 60 days after differentiation (control, 54.8 ± 3.5; R218W, 58.6 ± 8.1; R67W, 52.1 ± 5.2; R218Q, 47.2 ± 3.7 ms, data are mean ± SEM). c. cFPD obtained from the control- (n=14) and ATS-iPSC-derived beating EBs (n=12–14) at 60 days after differentiation (control, 447.1 ± 29.3; R218W, 529.5 ± 27.3; R67W, 492.2 ± 52.0; R218Q, 459.8 ± 26.3 ms, data are mean ± SEM). d, e, f, g. Representative recordings of action potential for iPSC-derived ventricular-type cardiomyocytes. h, i, j. Statistical parameters of action potential duration at 50% repolarization (APD_{50}) (control, n=13, 341.1 ± 22.8; R218W, n=10, 343.5 ± 27.2; R67W, n=12, 351.0 ± 29.6; R218Q, n=6, 397.0 ± 28.9 ms), 90% repolarization (APD_{90}) (control, 403.7 ± 26.2; R218W, 409.1 ± 30.4; R67W, 417.2 ± 32.7; R218Q, 490.0 ± 32.8 ms), and maximum diastolic potential (MDP) (control, −58.0 ± 2.0; R218W, −55.9 ± 1.7; R67W, −57.4 ± 1.5; R218Q, −52.3 ± 3.6mv) respectively. Data are mean ± SEM.

(τ) between control- and ATS-iPSC-derived cardiomyocytes (Figs. 5e, 5f, 5g). To know whether irregular Ca^{2+} release reflects on the increased diastolic cytosolic Ca^{2+} concentration, we tested pharmacological sarco/endoplasmic reticulum Ca^{2+}-ATPase (SERCA) inhibitor, cyclopiazonic acid (CPA), to increase the diastolic cytosolic Ca^{2+} concentration. CPA significantly increased the proportion of cardiomyocytes with irregular Ca^{2+} release in the control-iPSC-derived population (Supplementary Fig. 5c). This suggests that irregular Ca^{2+} release could be caused by diastolic Ca^{2+} overload. Next we quantified sarcoplasmic reticulum (SR) Ca^{2+} content, because this could affect cytosolic Ca^{2+} concentration [33]. SR Ca^{2+} content can be measured by the height of the Ca^{2+} transient induced by rapid caffeine application, which showed no significant difference in SR Ca^{2+} content between control- and ATS-iPSC-derived cardiomyocytes (Supplementary Fig. 5d, h). The calcium dynamics in cardiomyocyte are regulated by various organelles and proteins, such as ryanodine receptor, and SERCA2a [34]. Then we examined SR Ca^{2+} content after administration of flecainide, but found no significant difference between control- and ATS-iPSC-derived cardiomyocytes (Supplementary Fig. 5e). To further investigate the mechanisms of flecainide effect on the arrhythmogenicity of ATS, we measured the effect of flecainide on intracellular Ca^{2+} dynamics in ATS-iPSC-derived single cardiomyocytes. At baseline, we often observed irregular Ca^{2+} release in ATS-iPSC-derived single cardiomyocytes, and this irregularity was significantly reduced by flecainide in ATS-iPSC-derived single cardiomyocytes (Figs. 5i–k, Supplementary Fig. 5f–i).

3.5. A reverse-mode Na^+/Ca^{2+} exchanger inhibitor suppresses abnormal calcium transients in ATS-iPSC-derived cardiomyocytes

Flecainide is a cardiac-specific fast-inward Na^+ current blocker, but has pleiotropic functions. To examine whether the antiarrhythmic mechanism of flecainide would be affected by a Na^+ current blocker, we tried other a second cardiac fast-inward Na^+ current blocker, pilisicainide [35]. Unlike with flecainide, pilsicainide administration did not show a therapeutic effect on isoproterenol-induced arrhythmic events in ATS-iPSC-derived cardiomyocytes at various concentrations of pilisicainide (Fig. 6a, b). These data suggested that flecainide might not exert its antiarrhythmic effects in ATS by the Na^+ current blocking effect. Calcium dynamics are also regulated by a Na^+/Ca^{2+} exchanger (NCX) in cardiomyocytes [34]. Thus, we tested the effects of pharmacological NCX inhibition by KB-R7943, which at high levels inhibits both the forward- and reverse-mode (Ca^{2+} in, Na^+ out) NCX, but lower KB-R7943 inhibits only reverse-mode NCX [36]. Reverse-mode NCX in turns augments calcium release from the sarcoplasmic reticulum through ryanodine receptors [37], and in our experiments, 500 nM KB-R7943 also suppressed the irregular Ca^{2+} release (Fig. 6c). We also used more specific compound to NCX reverse mode, SEA0400 which reduced the incidence of cells with irregular Ca^{2+} release (Supplementary Fig. 6a, Supplementary Table 3). These results are similar to those obtained by flecainide administration. To know the involvement of RyR2, we examined the effect of JTV519 on the incidence of cells with irregular Ca^{2+} release but we did not find any difference in the incidence of cells with irregular Ca^{2+} release by JTV519 addition (Supplementary Fig. 6b).

3.6. Flecainide has a direct effect on NCX current

To elucidate the direct effect of flecainide on I_{NCX}, the whole-cell voltage-clamp experiment was conducted in isolated guinea-pig ventricular cardiomyocytes. I_{NCX} was induced by 1 mM Ca^{2+} and 140 mM Na^+ in the external solution and 20 mM Na^+ and 226 nM free Ca^{2+} in the pipette solution. Under these ionic conditions, the reversal potential of I_{NCX} with a 3Na:1Ca stoichiometry was calculated to be −68 mV. After establishing the whole-cell clamp mode, the external solution was changed to the control external solution. When the

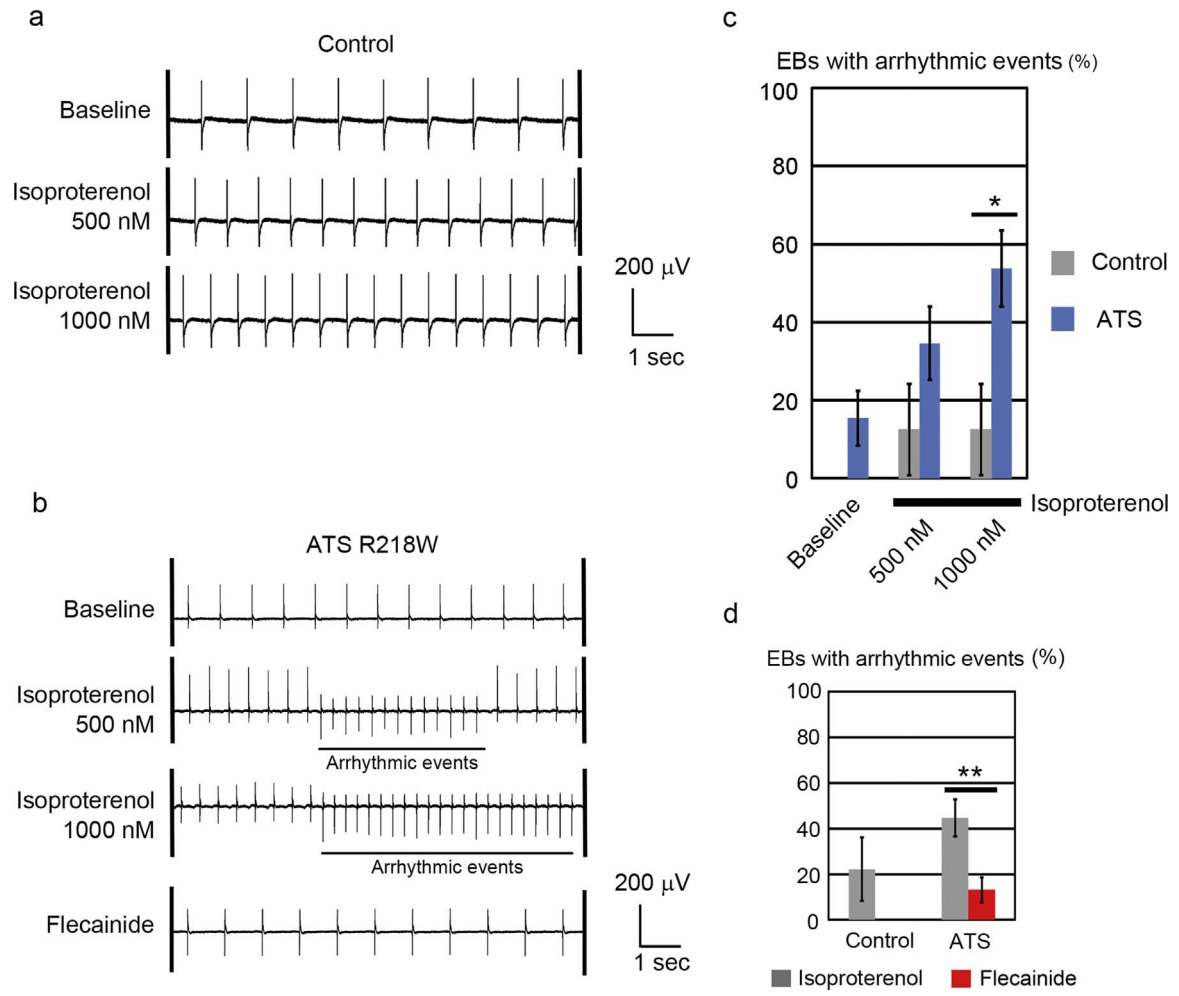

Fig. 4. Isoproterenol responses of ATS-iPSC-derived cardiomyocytes, a. Representative MEA recordings showing increased beating rates after isoproterenol administration in control-iPSC-derived beating EBs. b. Representative MEA recordings after isoproterenol and flecainide administration in ATS-iPSC-derived beating EBs. c. The rates of EBs with arrhythmic events in MEA analyses (control, n =8; ATS, n=26, $^{*}P < 0.05$ vs. control by Fisher's exact probability test). d. The incidences of EBs with arrhythmic events after isoproterenol (1000 nM) and flecainide (5 μM) administration by MEA analysis (control, n=9; ATS, n=38, $^{**}P < 0.01$ by Fisher's exact probability test).

external solution was switched to one containing 30 μM flecainide, I_{NCX} was immediately augmented (Fig. 7a), although 5 mM of Ni, a potent and selective inhibitor of I_{NCX} under the present conditions, was applied to completely inhibit I_{NCX}. The I–V curves of flecainide-sensitive (a–c) and Ni-sensitive (b–c) components were obtained by subtraction (Fig. 7b). Both I-V curves are reversed at about −65 mV, indicating that the flecainide-sensitive current is I_{NCX}. Flecainide therefore augmented the bi-directional I_{NCX} in a concentration-dependent manner (Figs. 7c-d).

4. Discussion

Human genetic studies have successfully revealed the causal genes and mechanisms of inheritable arrhythmic disease [38]. Subsequent in vitro experiments using a heterologous expression system revealed the electrophysiological properties of wild-type and mutated ion channel, while genetically modified mice have played an important role in elucidating the *in vivo* function of specific genes [39], including in arrhythmic diseases [40]. However, mouse models of human arrhythmic diseases have several limitations. Compared to humans, the mouse has a small heart, a high basal heart rate, a short action potential of ventricular cardiomyocytes, and differential roles for some ion currents [41], and thus, many inheritable arrhythmic diseases cannot be modeled in mouse.

KCNJ2 mutations in ATS1 mostly decrease I_{K1} in vitro, thus affecting action potential repolarization and resting potential stabilization [17,18]. *In ex vivo* canine heart tissue, I_{K1} blockade by CsCl induced DADs and polymorphic ventricular tachycardia (VT) [42], while *in ex vivo* guinea pig heart, I_{K1} blockade by $BaCl_2$ induced high susceptibility to arrhythmic events in hypokalemic conditions due to cytosolic calcium accumulation [43]. *In ex vivo* rabbit heart, I_{K1} blockade by CsCl induced bidirectional ventricular tachycardia due to beat-to-beat alteration at the diastolic calcium content and triggered activity [44]. Although such drug-induced disease models are simple and useful, many drugs have pleiotropic effects and in elucidating specific gene functions *in vivo*, it is preferable to generate genetically modified disease models resembling human disease.

Many *KCNJ2* mutations in patients with ATS1 have dominant-negative effects on I_{K1} [45]. To decipher the role of Kir2.1 in cardiomyocytes in vivo, several genetically modified models were generated, with the first *KCNJ2* knockout mice showing early lethality at the perinatal period due to a complete cleft of the secondary palate, and that *KCNJ2* is required for I_{K1}- and K^+-induced dilations in cerebral arteries [46]. In addition, cardiac-specific overexpression of a dominant-negative *KCNJ2* in mice reduces I_{K1} reduction by 95%, leading to a significant prolongation of action potentials [47]. *KCNJ2*-knockout ventricular cardiomyocytes lack detectable I_{K1} and show significantly broader action potentials and more frequent spontaneous action potentials than wild-type myocytes [48]. However, *KCNJ2* knockout neonates show neither ectopic beats nor re-entry arrhyth-

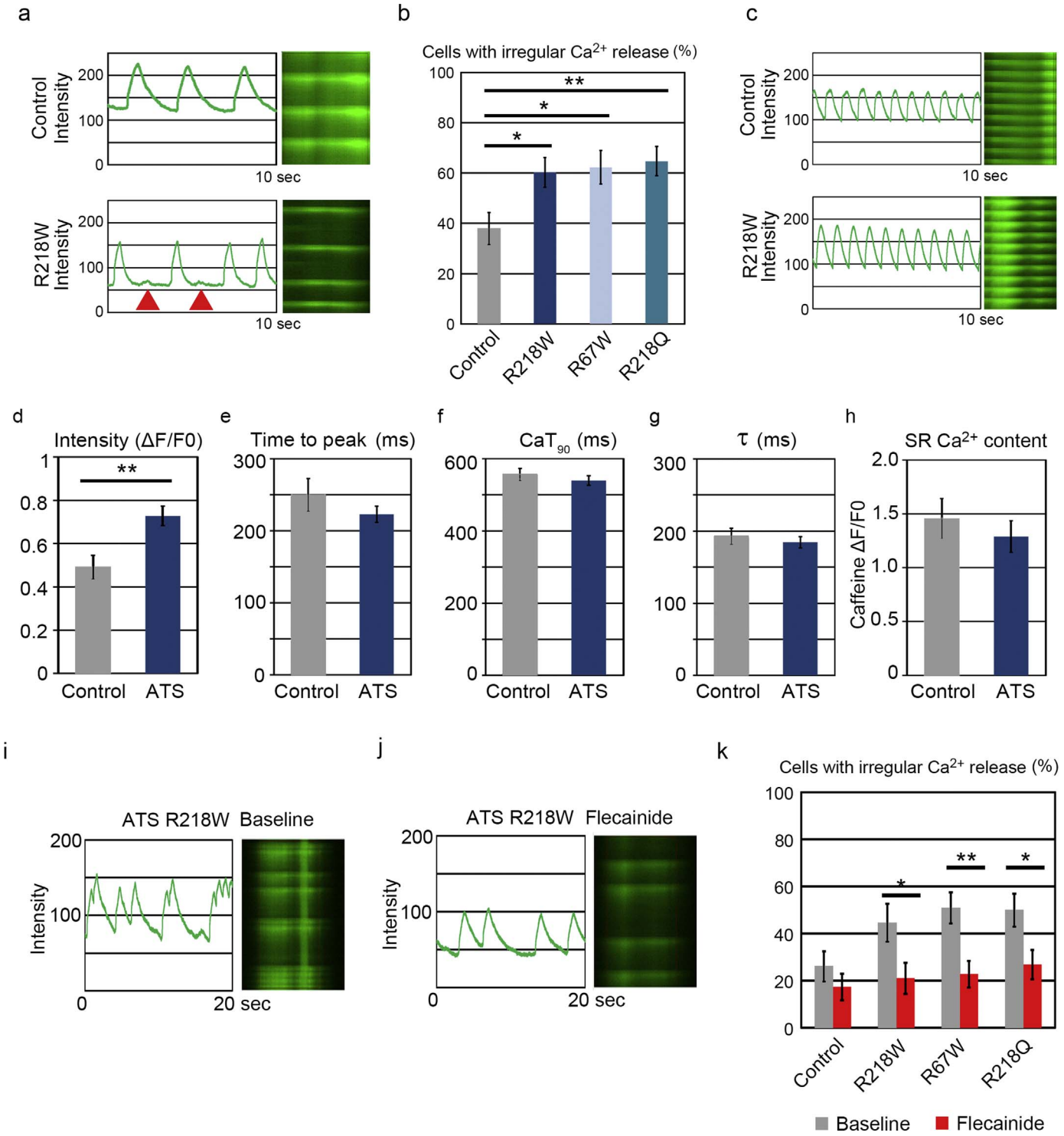

Fig. 5. Ca^{2+} transients of ATS-iPSC-derived cardiomyocytes, a. Representative line scan images of spontaneous Ca^{2+} transients in control- and ATS-iPSC-derived single cardiomyocytes. Arrowhead indicates the irregular Ca^{2+} release. b. The incidences of cardiomyocytes with irregular Ca^{2+} release at the baseline condition (control, n=58, 37.9%; ATS, R218W, n=68, 60.3%, R67W, n=53, 62.3%, R218Q, n=68, 64.7%, $*P < 0.05$, $**P < 0.01$ vs. control by Chi-square test). c. Representative line scan images of Ca^{2+} transients paced at 1 Hz in control- and ATS-iPSC-derived single cardiomyocytes. d, e, f, g. Statistical parameters of Ca^{2+} transient intensity (ΔF/F0) (d), time to peak (e), time to 90% decay of the Ca^{2+} transient (CaT_{90}) (f), and of Ca^{2+} transient decline (τ) (g), $**P < 0.01$ vs. control by student's *t*-test. in control- (n=22) and ATS-iPSC-derived cardiomyocytes (n=54). Data are mean ± SEM. h. SR Ca^{2+} content was determined by the caffeine-induced ΔF/F0 (F0 is the baseline fluorescence and ΔF is the baseline subtracted fluorescence.) (control, n =6, 1.46 ± 0.19; ATS, n =7, 1.29 ± 0.15, $**P < 0.01$ vs. control by Student's *t*-test, Data are mean ± SEM.). i. Representative line scan images of spontaneous Ca^{2+} transients at baseline in ATS-iPSC-derived single cardiomyocytes. j. Representative line scan images of spontaneous Ca^{2+} transients after flecainide (500 nM) administration in ATS-iPSC-derived single cardiomyocytes. k. The incidences of cardiomyocytes with irregular Ca^{2+} release after flecainide administration (control, n=46, 8.7% decrease in incidence; ATS, R218W, n=38, R67W, n=57, R218Q, n=52, 23.6%, 28.1%, 23.1% decreases in incidence, respectively, $*P < 0.05$, $**P < 0.01$ vs. baseline by Fisher's exact probability test).

mias, suggesting that the increased automaticity and prolonged action potential were not sufficient causes of arrhythmic events in these mice. These results suggest that genetically modified mice could not fully recapitulate the phenotype of patients with ATS1.

ATS-iPSC-derived cardiomyocytes generated in the current study showed a significantly higher incidence of irregular Ca^{2+} release. Drug

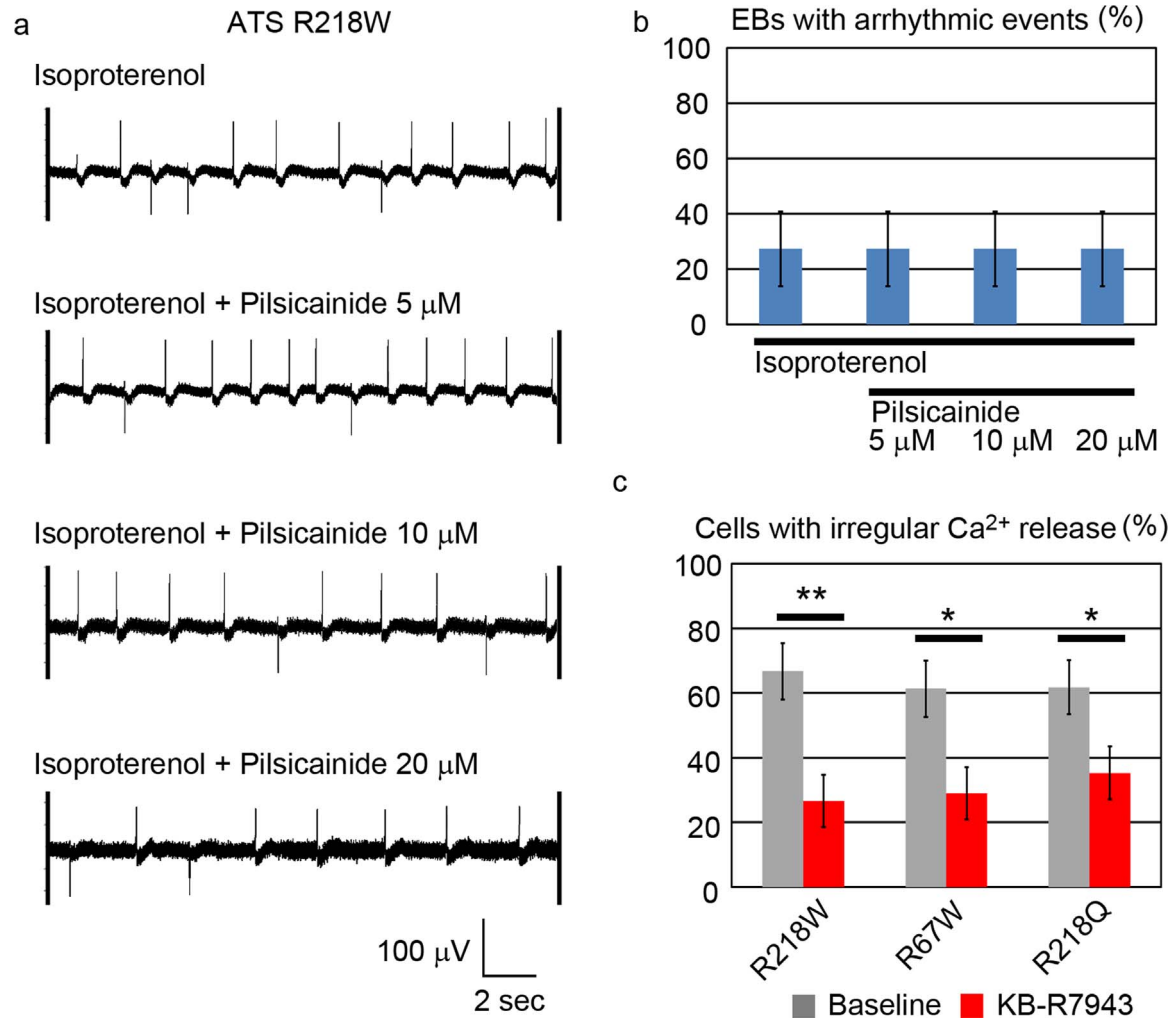

Fig. 6. Therapeutic electrophysiological pathway of ATS-iPSC-derived cardiomyocytes, a. Representative MEA recordings showing the arrhythmic events after isoproterenol and pilsicainide administration in ATS-iPSC-derived cardiomyocytes. b. The incidences of EBs with arrhythmic events after isoproterenol and pilsicainide administration in MEA analysis (n=11). c. The incidences of cardiomyocytes with irregular Ca^{2+} release after KB-R7943 administration (R218W, n =30, R67W, n=31, R218Q, n=34, 40.0%, 32.3%, 26.5% decreases in incidence, respectively. $^{*}P < 0.05$, $^{**}P < 0.01$ vs. baseline by Fisher's exact probability test).

testing revealed that irregular Ca^{2+} release and arrhythmic events were significantly suppressed by flecainide, but not by a pure sodium channel blocker, pilsicainide. Flecainide blocks the cardiac fast-inward Na^{+} current [49], but has pleiotropic functions such as inhibiting the rapid component of the delayed rectifier K^{+} current [50], the late Na^{+} current [51], and cardiac ryanodine receptor-mediated Ca^{2+} release [33]. Indeed, a drug-induced ATS model in guinea pig heart showed that higher NCX expression and weaker SERCA2a expression correlated with arrhythmic events, and that NCX inhibition by 5 μM KB-R7943 decreased arrhythmic events [52]. This concentration of KB-R7943 fully inhibits both forward-mode and reverse-mode NCX, while lower concentrations inhibit reverse-mode, but not forward-mode, NCX [53]. Reverse-mode NCX augments calcium release from the sarcoplasmic reticulum through ryanodine receptors [37], while inhibiting forward-mode NCX augments cytosolic Ca^{2+} overload [54]. If the antiarrhythmic effect of flecainide and KB-R7943 works by blocking forward-mode NCX, irregular Ca^{2+} release would not be decreased in ATS-iPSC-derived cardiomyocytes. In contrast, treatment of our ATS-iPSC-derived cardiomyocytes with flecainide and 500 nM KB-R7943 sufficiently suppressed both the increased arrhythmic events and irregular Ca^{2+} release, while flecainide also augmented the bi-directional I_{NCX}. These results support the notion that direct I_{NCX} modulation would successfully suppress an arrhythmogenic substrate in ATS-iPSC-derived cardiomyocytes. Previous report showed that flecainide reduces I_{Na}, which results in increased Ca^{2+} efflux via NCX across the sarcolemma [55]. We could not observed anti-arrhythmic effect by other sodium channel blocker in ATS-iPSC-derived cardiomyocytes. In our experimental condition, both flecainide and a reverse-mode NCX inhibitor reduced the arrhythmic events, and flecainide augmented the bi-directional I_{NCX}.

NCX is the main pathway for Ca^{2+} efflux from cardiomyocytes [56,57]. Ca^{2+} removal through the forward mode produces an inward current, while the reverse mode bringing Ca^{2+} into the cardiomyocytes produces an outward current. In fact, the mode of NCX dynamically changes throughout the cardiomyocyte cycle, although under normal conditions, net NCX activity in cardiomyocytes uses the forward mode. Now it seems that NCX might have a dual role in arrhythmogenesis. Firstly, reverse-mode NCX is the principal pathway that loads the cardiomyocytes with Ca^{2+} and causes Ca^{2+} overload. Secondly, the forward mode carries the inward current of a DAD. Thus, balancing the NCX mode in cardiomyocytes would be critical for electrophysiolgical homeostasis. In the ATS-iPSC-derived cardiomyocytes, we observed an increased rate of irregular Ca^{2+} release, prompting the speculation that inhibiting reverse-mode NCX would reduce Ca^{2+} overload, following an antiarrhythmic effect. Low-dose KB-R7943 also successfully reduced arrhythmic events in our study, thus we hypothesized that flecainide would have a role in reverse-mode NCX inhibition. Of interest, flecainide induced the augmentation of I_{NCX} in both modes, and in

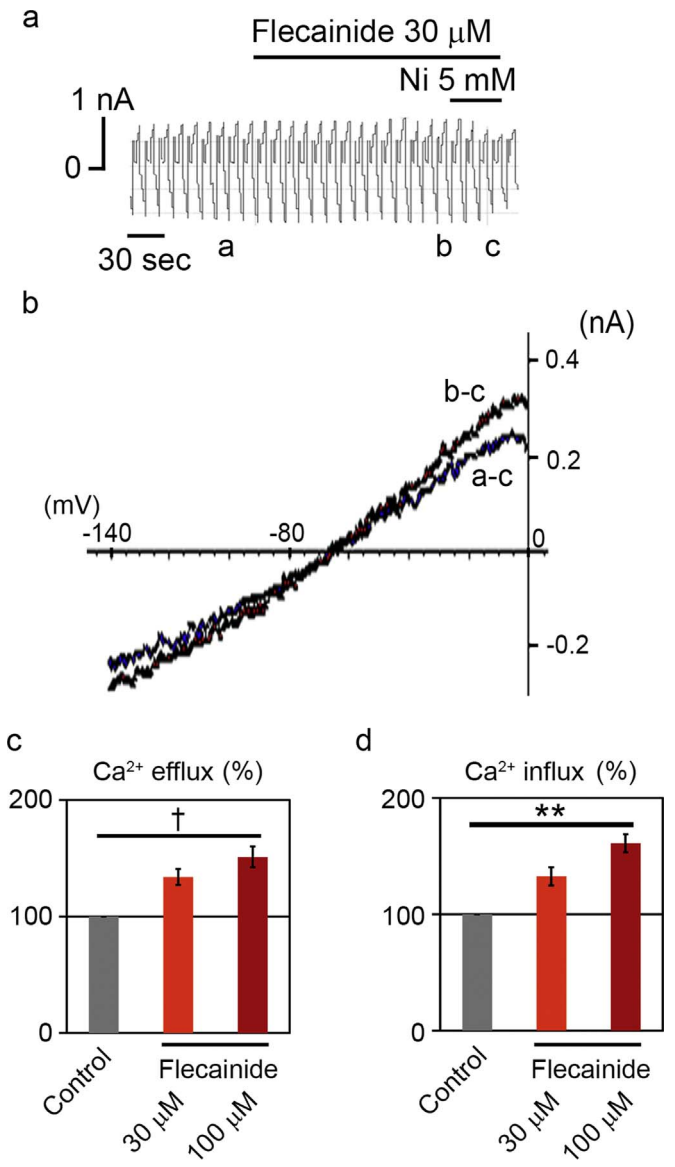

Fig. 7. Effect of flecainide on I_{NCX}. a. Representative chart recording of membrane current. The horizontal bars above the current indicate when 30 μM flecainide and 5 mM Ni were applied externally. b. I-V curves obtained at the corresponding labels in panel a. a, control; b, in the presence of flecainide; c, in the presence of Ni. c. Summarized data of the augmentation effect of 30 μM and 100 μM flecainide on bi-directional I_{NCX}. (Ca efflux mode; 33.8 ± 6.8% increase in I_{NCX} at 30 μM flecainide and 51.0 ± 8.9% increase in I_{NCX} at 100 μM flecainide, Ca influx mode; 32.4 ± 7.7% increase in I_{NCX} at 30 μM flecainide and 61.0 ± 8.0% increase in I_{NCX} at 100 μM flecainide, $^{**}P < 0.01$, $^{\dagger}P < 0.001$ vs. control by paired *t*-test; values are means ± SEM. of 5 cells).

cycling cardiomyocytes, the forward-mode and reverse-mode are balanced. An increased I_{NCX} would increase the net forward-mode I_{NCX}, resembling the effect of reverse-mode NCX inhibition.

There are some limitations in this study. The iPSC-derived cardiomyocytes used herein showed an immature phenotype. Unfortunately, despite on-going attempts to obtain mature iPSC-derived cardiomyocytes resembling adult rod-shape cardiomyocytes, current techniques do not accomplish full maturation. We used three unrelated patients with ATS and two unrelated healthy volunteers as controls, all with totally different genetic backgrounds, which can potentially affect disease phenotype. It is therefore preferable to use isogenic control iPSCs generated by gene correction. In this study, we focused on the common phenotype of three patients with ATS that was not observed in two controls. I_{K1} is very small in iPSC-derived cardiomyocytes, and it is difficult to show the clear difference between patient- and control-derived cells by a patch clamp technique, especially with respect to the loss of function phenotype. But interestingly, we uncovered the electrophysiological findings of ATS-iPSC-derived cardiomyocytes by MEA analysis and Ca^{2+} imaging. KB-R7943 is not a specific inhibitor for NCX, and there are more selective inhibitors available, such as SEA-0400 and SN-6. Thus a higher dose of KB-R7943 could inhibit fast Na^{+}, L-type Ca^{2+}, inward-rectifier and delayed K^{+} currents in the micromolar range [58], although we used lower concentration of KB-R7943 to minimize such effects. We used flecainide at relatively high concentration for guinea pig experiments. This experiment showed a possible new mechanism of flecainide for NCX augmentation and it remain elusive whether NCX effect solely shows the therapeutic potential on ATS. The underlying precise mechanism for the irregular Ca^{2+} releases and arrhythmogenic beating of ATS-iPSC-derived cardiomyocytes remains unclear. In supplementary Fig. 5c, we induced cytosolic Ca^{2+} overload by SERCA inhibition using CPA and the incidence of irregular Ca^{2+} release is increased, which suggests that irregular Ca^{2+} releases in ATS-iPSC-derived cardiomyocytes might be induced by Ca^{2+} overload. We speculated that I_{K1} reduction would result in destabilization of resting membrane potential and depolarized resting membrane potential affects the kinetics of L-type Ca^{2+} channel to augment Ca^{2+} influx [59], which results in Ca^{2+} overload. Ca^{2+} efflux through NCX reverse mode would generate I_{TI}, which result in the appearance of DAD.

The rarity of ATS makes it difficult to analyze disease pathogenesis in humans to develop novel therapeutics. In this study we established a disease model of ATS using patient-specific iPSCs. Such iPSCs could be stored and maintained in a cell bank facility, with future efforts recruiting many more patients to facilitate future drug screening. Arrhythmic events in MEA analysis and irregular Ca^{2+} releases in Ca^{2+} imaging might provide pathogenic hallmarks of ATS-iPSC-derived cardiomyocytes that could in turn be used in high-throughput, automated approaches to drug screening. Flecainide and a reverse-mode NCX inhibitor successfully decreased the incidence of arrhythmic events in ATS-iPSC-derived cardiomyocytes. Finally, we uncovered an unexpected effect of flecainide, I_{NCX} augmentation, which could offer new therapeutic targets for ATS and other such conditions.

Disclosures

None.

Competing financial interests

K.F. is a Founding Scientist and a paid SAB of Heartseed Co. Ltd.

Acknowledgments

The authors thank all the laboratory members for their critical comments and helpful discussions. The authors thank Drs. I. Komuro, H. Morita and A. Naito (University of Tokyo) for helpful discussions. This study was supported, in part, by research grants from the Program for Intractable Diseases Research utilizing Disease-specific iPS cells from Japan Agency for Medical Research and development, AMED, Grants-in-Aid for Scientific Research (JSPS KAKENHI Grant Number: 26670408, 15H01521, 16H050304, 16K15415), a Health Labour Sciences Research Grant, the New Energy and Industrial Technology Development Organization, and the Program for Promotion of Fundamental Studies in Health Science of the National Institute of Biomedical Innovation, Suzuken Memorial Foundation and Keio University Medical Science Fund.

Appendix A. Transparency document

Transparency document associated with this article can be found in the online version at http://dx.doi.org/10.1016/j.bbrep.2017.01.002.

References

[1] E.D. Andersen, P.A. Krasilnikoff, H. Overvad, Intermittent muscular weakness, extrasystoles, and multiple developmental anomalies. A new syndrome?, Acta Paediatr. Scand. 60 (1971) 559–564.

[2] R. Tawil, L.J. Ptacek, S.G. Pavlakis, D.C. DeVivo, A.S. Penn, C. Ozdemir, R.C. Griggs, Andersen's syndrome: potassium-sensitive periodic paralysis, ventricular ectopy, and dysmorphic features, Ann. Neurol. 35 (1994) 326–330.

[3] M. Tristani-Firouzi, J.L. Jensen, M.R. Donaldson, V. Sansone, G. Meola, A. Hahn, S. Bendahhou, H. Kwiecinski, A. Fidzianska, N. Plaster, Y.H. Fu, L.J. Ptacek, R. Tawil, Functional and clinical characterization of KCNJ2 mutations associated with LQT7 (Andersen syndrome), J. Clin. Investig. 110 (2002) 381–388.

[4] L. Zhang, D.W. Benson, M. Tristani-Firouzi, L.J. Ptacek, R. Tawil, P.J. Schwartz, A.L. George, M. Horie, G. Andelfinger, G.L. Snow, Y.-H. Fu, M.J. Ackerman, G.M. Vincent, Electrocardiographic features in Andersen-Tawil syndrome patients with KCNJ2 mutations: characteristic T-U–wave patterns predict the KCNJ2 genotype, Circulation 111 (2005) 2720–2726.

[5] E. Delannoy, F. Sacher, P. Maury, P. Mabo, J. Mansourati, I. Magnin, J.-P. Camous, G. Tournant, E. Rendu, F. Kyndt, M. Haïssaguerre, S. Bézieau, B. Guyomarch, H. Le Marec, V. Fressart, I. Denjoy, V. Probst, Cardiac characteristics and long-term outcome in Andersen–Tawil syndrome patients related to KCNJ2 mutation, Europace 15 (2013) 1805–1811.

[6] A.H. Smith, F.A. Fish, P.J. Kannankeril, Andersen-Tawil syndrome, Indian Pacing Electro. J. 6 (2006) 32–43.

[7] R. Bökenkamp, A.A. Wilde, M.J. Schalij, N.A. Blom, Flecainide for recurrent malignant ventricular arrhythmias in two siblings with Andersen-Tawil syndrome, Heart Rhythm 4 (2007) 508–511.

[8] P.J. Kannankeril, D.M. Roden, F.A. Fish, Suppression of bidirectional ventricular tachycardia and unmasking of prolonged QT interval with Verapamil in Andersen's Syndrome, J. Cardiovasc. Electrophysiol. 15 (2004) (119-119).

[9] J. Junker, W. Haverkamp, E. Schulze-Bahr, L. Eckardt, W. Paulus, R. Kiefer, Amiodarone and acetazolamide for the treatment of genetically confirmed severe Andersen syndrome, Neurology 59 (2002) 466.

[10] S. Peters, E. Schulze-Bahr, S.P. Etheridge, M. Tristani-Firouzi, Sudden cardiac death in Andersen–Tawil syndrome, Europace 9 (2007) 162–166.

[11] A.A.M. Wilde, Andersen–Tawil Syndrome, Scarier for the Doctor than for the Patient? Who, When, and How to Treat, Europace, 15, 2013, pp. 1690–1692.

[12] M.F. Márquez, S. Nava, J. Gómez, L. Colín, P. Iturralde, Lack of efficacy of radiofrequency catheter ablation in Andersen–Tawil syndrome: are we targeting the right spot?, Europace (2014).

[13] N.M. Plaster, R. Tawil, M. Tristani-Firouzi, S. Canún, Sd Bendahhou, A. Tsunoda, M.R. Donaldson, S.T. Iannaccone, E. Brunt, R. Barohn, J. Clark, F. Deymeer, A.L. George Jr, F.A. Fish, A. Hahn, A. Nitu, C. Ozdemir, P. Serdaroglu, S.H. Subramony, G. Wolfe, Y.-H. Fu, L.J. Ptáček, Mutations in Kir2.1 cause the developmental and episodic electrical phenotypes of Andersen's syndrome, Cell 105 (2001) 511–519.

[14] H.-L. Nguyen, G.H. Pieper, R. Wilders, Andersen–Tawil syndrome: clinical and molecular aspects, Int. J. Cardiol. 170 (2013) 1–16.

[15] T. Ai, Y. Fujiwara, K. Tsuji, H. Otani, S. Nakano, Y. Kubo, M. Horie, Novel KCNJ2 mutation in familial periodic paralysis with ventricular dysrhythmia, Circulation 105 (2002) 2592–2594.

[16] R. Preisig-Müller, G. Schlichthörl, T. Goerge, S. Heinen, A. Brüggemann, S. Rajan, C. Derst, R.W. Veh, J. Daut, Heteromerization of Kir2.x potassium channels contributes to the phenotype of Andersen's syndrome, in: Proceedings of the National Academy of Sciences, 99, 2002, pp. 7774–7779.

[17] A.N. Lopatin, C.G. Nichols, Inward rectifiers in the heart: an update on IK1, J. Mol. Cell. Cardiol. 33 (2001) 625–638.

[18] Z. Wang, L. Yue, M. White, G. Pelletier, S. Nattel, Differential distribution of inward rectifier potassium channel transcripts in human atrium versus ventricle, Circulation 98 (1998) 2422–2428.

[19] R.J. Sung, S.N. Wu, J.S. Wu, H.D. Chang, C.H. Luo, Electrophysiological mechanisms of ventricular arrhythmias in relation to Andersen-Tawil syndrome under conditions of reduced IK1: a simulation study, Am. J. Physiol. Heart Circ. Physiol. 291 (2006) H2597–H2605.

[20] T. Egashira, S. Yuasa, T. Suzuki, Y. Aizawa, H. Yamakawa, T. Matsuhashi, Y. Ohno, S. Tohyama, S. Okata, T. Seki, Y. Kuroda, K. Yae, H. Hashimoto, T. Tanaka, F. Hattori, T. Sato, S. Miyoshi, S. Takatsuki, M. Murata, J. Kurokawa, T. Furukawa, N. Makita, T. Aiba, W. Shimizu, M. Horie, K. Kamiya, I. Kodama, S. Ogawa, K. Fukuda, Disease characterization using LQTS-specific induced pluripotent stem cells, Cardiovasc. Res. 95 (2012) 419–429.

[21] A. Tanaka, S. Yuasa, G. Mearini, T. Egashira, T. Seki, M. Kodaira, D. Kusumoto, Y. Kuroda, S. Okata, T. Suzuki, T. Inohara, T. Arimura, S. Makino, K. Kimura, A. Kimura, T. Furukawa, L. Carrier, K. Node, K. Fukuda, Endothelin-1 induces myofibrillar disarray and contractile vector variability in hypertrophic cardiomyopathy–induced pluripotent stem cell–derived cardiomyocytes, J. Am. Heart Assoc. 3 (2014).

[22] S. Okata, S. Yuasa, T. Suzuki, S. Ito, N. Makita, T. Yoshida, M. Li, J. Kurokawa, T. Seki, T. Egashira, Y. Aizawa, M. Kodaira, C. Motoda, G. Yozu, M. Shimojima, N. Hayashiji, H. Hashimoto, Y. Kuroda, A. Tanaka, M. Murata, T. Aiba, W. Shimizu, M. Horie, K. Kamiya, T. Furukawa, K. Fukuda, Embryonic type Na+ channel β-subunit, SCN3B masks the disease phenotype of Brugada syndrome, Sci. Rep. 6 (2016) 34198.

[23] M. Kodaira, H. Hatakeyama, S. Yuasa, T. Seki, T. Egashira, S. Tohyama, Y. Kuroda, A. Tanaka, S. Okata, H. Hashimoto, D. Kusumoto, A. Kunitomi, M. Takei, S. Kashimura, T. Suzuki, G. Yozu, M. Shimojima, C. Motoda, N. Hayashiji, Y. Saito, Y.-i. Goto, K. Fukuda, Impaired respiratory function in MELAS-induced pluripotent stem cells with high heteroplasmy levels, FEBS Open Bio. 5 (2015) 219–225.

[24] A. Tanaka, S. Yuasa, K. Node, K. Fukuda, Cardiovascular disease modeling using patient-specific induced pluripotent stem cells, Int. J. Mol. Sci. 16 (2015) 18894.

[25] T. Seki, S. Yuasa, K. Fukuda, Generation of induced pluripotent stem cells from a small amount of human peripheral blood using a combination of activated T cells and Sendai virus, Nat, Protocols 7 (2012) 718–728.

[26] T. Seki, S. Yuasa, K. Fukuda, Derivation of Induced Pluripotent Stem Cells from Human Peripheral Circulating T Cells, John Wiley & Sons, Inc, 2011 (Current Protocols in Stem Cell Biology).

[27] Y. Hosaka, H. Hanawa, T. Washizuka, M. Chinushi, F. Yamashita, T. Yoshida, S. Komura, H. Watanabe, Y. Aizawa, Function, subcellular localization and assembly of a novel mutation of KCNJ2 in Andersen's syndrome, J. Mol. Cell. Cardiol. 35 (2003) 409–415.

[28] T. Egashira, S. Yuasa, S. Tohyama, Y. Kuroda, T. Suzuki, T. Seki, K. Fukuda, Patient-specific induced pluripotent stem cell models: characterization of iPS cell-derived cardiomyocytes, in: A. Nagy, K. Turksen (Eds.), Patient-Specific Induced Pluripotent Stem Cell Models, Generation and Characterization, Springer New York, New York, NY, 2016, pp. 343–353.

[29] T. Seki, S. Yuasa, D. Kusumoto, A. Kunitomi, Y. Saito, S. Tohyama, K. Yae, Y. Kishino, M. Okada, H. Hashimoto, M. Takei, T. Egashira, M. Kodaira, Y. Kuroda, A. Tanaka, S. Okata, T. Suzuki, M. Murata, J. Fujita, K. Fukuda, Generation and characterization of functional cardiomyocytes derived from human T cell-derived induced pluripotent stem cells, PLOS ONE 9 (2014) e85645.

[30] A. Moretti, M. Bellin, A. Welling, C.B. Jung, J.T. Lam, L. Bott-Flügel, T. Dorn, A. Goedel, C. Höhnke, F. Hofmann, M. Seyfarth, D. Sinnecker, A. Schömig, K.-L. Laugwitz, Patient-specific induced pluripotent stem-cell models for long-QT syndrome, New Engl. J. Med. 363 (2010) 1397–1409.

[31] T. Yamakawa, Y. Watanabe, H. Watanabe, J. Kimura, Inhibitory effect of cibenzoline on Na+/Ca2+ exchange current in guinea-pig cardiac ventricular myocytes, J. Pharmacol. Sci. 120 (2012) 59–62.

[32] T. Seki, S. Yuasa, M. Oda, T. Egashira, K. Yae, D. Kusumoto, H. Nakata, S. Tohyama, H. Hashimoto, M. Kodaira, Y. Okada, H. Seimiya, N. Fusaki, M. Hasegawa, K. Fukuda, Generation of induced pluripotent stem cells from human terminally differentiated circulating T cells, Cell Stem Cell 7 (2010) 11–14.

[33] H. Watanabe, N. Chopra, D. Laver, H.S. Hwang, S.S. Davies, D.E. Roach, H.J. Duff, D.M. Roden, A.A.M. Wilde, B.C. Knollmann, Flecainide prevents catecholaminergic polymorphic ventricular tachycardia in mice and humans, Nat. Med. 15 (2009) 380–383.

[34] D.M. Bers, Calcium fluxes involved in control of cardiac myocyte contraction, Circ. Res. 87 (2000) 275–281.

[35] T. Yamashita, Y. Murakawa, K. Sezaki, N. Hayami, M. Inoue, E. Fukui, M. Omata, Uniqueness of pilsicainide in class Ic antiarrhythmics, Jpn. Heart J. 39 (1998) 389–397.

[36] T. Iwamoto, T. Watano, M. Shigekawa, A. Novel Isothiourea, Derivative selectively inhibits the reverse mode of Na+/Ca2+ exchange in cells expressing NCX1, J. Biol. Chem. 271 (1996) 22391–22397.

[37] R. Larbig, N. Torres, J.H.B. Bridge, J.I. Goldhaber, K.D. Philipson, Activation of reverse Na+–Ca2+ exchange by the Na+ current augments the cardiac Ca2+ transient: evidence from NCX knockout mice, J. Physiol. 588 (2010) 3267–3276.

[38] M.T. Keating, M.C. Sanguinetti, Molecular and cellular mechanisms of cardiac arrhythmias, Cell 104 (2001) 569–580.

[39] G. Vogel, A knockout award in medicine, Science 318 (2007) 178–179.

[40] X.H.T. Wehrens, S.E. Lehnart, F. Huang, J.A. Vest, S.R. Reiken, P.J. Mohler, J. Sun, S. Guatimosim, L.-S. Song, N. Rosemblit, J.M. D'Armiento, C. Napolitano, M. Memmi, S.G. Priori, W.J. Lederer, A.R. Marks, FKBP12.6 deficiency and defective calcium release channel (ryanodine receptor) function linked to exercise-induced sudden cardiac death, Cell 113 (2003) 829–840.

[41] D.J. Milan, C.A. MacRae, Animal models for arrhythmias, Cardiovasc. Res. 67 (2005) 426–437.

[42] H. Morita, D.P. Zipes, S.T. Morita, J. Wu, Mechanism of U wave and polymorphic ventricular tachycardia in a canine tissue model of Andersen–Tawil syndrome, Cardiovasc. Res. 75 (2007) 510–518.

[43] S. Poelzing, R. Veeraraghavan, Heterogeneous ventricular chamber response to hypokalemia and inward rectifier potassium channel blockade underlies bifurcated T wave in guinea pig, Am. J. Physiol. - Heart Circ. Physiol. 292 (2007) H3043–H3051.

[44] M. Maruyama, S.-F. Lin, P.-S. Chen, Alternans of diastolic intracellular calcium elevation as the mechanism of bidirectional ventricular tachycardia in a rabbit model of Andersen-Tawil syndrome, Heart Rhythm 9 (2012) 626–627.

[45] P.S. Lange, F. Er, N. Gassanov, U.C. Hoppe, Andersen mutations of KCNJ2 suppress the native inward rectifier current IK1 in a dominant-negative fashion, Cardiovasc. Res. 59 (2003) 321–327.

[46] J.J. Zaritsky, D.M. Eckman, G.C. Wellman, M.T. Nelson, T.L. Schwarz, Targeted disruption of Kir2.1 and Kir2.2 genes reveals the essential role of the inwardly rectifying K+ current in K+-mediated vasodilation, Circ. Res. 87 (2000) 160–166.

[47] M. McLerie, A. Lopatin, Dominant-negative suppression of IK1 in the mouse heart leads to altered cardiac excitability, J. Mol. Cell. Cardiol. 35 (2003) 367–378.

[48] J.J. Zaritsky, J.B. Redell, B.L. Tempel, T.L. Schwarz, The consequences of disrupting cardiac inwardly rectifying K+ current (IK1) as revealed by the targeted deletion of the murine Kir2.1 and Kir2.2 genes, J. Physiol. 533 (2001) 697–710.

[49] E. Aliot, A. Capucci, H.J. Crijns, A. Goette, J. Tamargo, Twenty-five years in the making: flecainide is safe and effective for the management of atrial fibrillation, Europace 13 (2011) 161–173.

[50] T. Anno, L.M. Hondeghem, Interactions of flecainide with guinea pig cardiac sodium channels. Importance of activation unblocking to the voltage dependence of

recovery, Circ. Res. 66 (1990) 789–803.
[51] J. Tamargo, R. Caballero, R. Gómez, C. Valenzuela, E. Delpón, Pharmacology of cardiac potassium channels, Cardiovasc. Res. 62 (2004) 9–33.
[52] P.B. Radwański, S. Poelzing, NCX is an important determinant for premature ventricular activity in a drug-induced model of Andersen–Tawil syndrome, Cardiovasc. Res. 92 (2011) 57–66.
[53] T. Watano, J. Kimura, T. Morita, H. Nakanishi, A novel antagonist, No. 7943, of the Na+/Ca2+ exchange current in guinea-pig cardiac ventricular cells, Br. J. Pharm. 119 (1996) 555–563.
[54] S. Ozdemir, V. Bito, P. Holemans, L. Vinet, J.-J. Mercadier, A. Varro, K.R. Sipido, Pharmacological inhibition of Na/Ca exchange results in increased cellular Ca2+ load attributable to the predominance of forward mode block, Circ. Res. 102 (2008) 1398–1405.
[55] M.B. Sikkel, T.P. Collins, C. Rowlands, M. Shah, P. O'Gara, A.J. Williams, S.E. Harding, A.R. Lyon, K.T. MacLeod, Flecainide reduces Ca2+ spark and wave frequency via inhibition of the sarcolemmal sodium current, Cardiovasc. Res. 98 (2013) 286–296.
[56] K.R. Sipido, A. Varro, D. Eisner, Sodium calcium exchange as a target for antiarrhythmic therapy, Handb. Exp. Pharm. (2006) 159–199.
[57] G. Antoons, K.R. Sipido, Targeting calcium handling in arrhythmias, Europace 10 (2008) 1364–1369.
[58] H. Tanaka, K. Nishimaru, T. Aikawa, W. Hirayama, Y. Tanaka, K. Shigenobu, Effect of SEA0400, a novel inhibitor of sodium-calcium exchanger, on myocardial ionic currents, Br. J. Pharmacol. 135 (2002) 1096–1100.
[59] R.J. Sung, S.-N. Wu, J.-S. Wu, H.-D. Chang, C.-H. Luo, Electrophysiological mechanisms of ventricular arrhythmias in relation to Andersen-Tawil syndrome under conditions of reduced IK1: a simulation study, Am. J. Physiol. -Heart Circ. Physiol. 291 (2006) H2597–H2605.